PCCP

Rotational quantum dynamics in a non-activated adsorption system

Arezoo Dianat and Axel Groß*

Physik-Department T30, Technische Universität München, D-85747, Garching, Germany. E-mail: agross@ph.tum.de

Received 5th April 2002, Accepted 24th June 2002
First published as an Advance Article on the web 25th July 2002

The effect of the rotational dynamics on the dissociation of hydrogen on Pd(100) has been studied by three- and five-dimensional quantum dynamical coupled-channel calculations. We have used a model potential energy surface with features derived from *ab initio* calculations. In particular, we have focused on the effect of the change of the hydrogen bond length upon adsorption and desorption which leads to a non-monotonic behaviour both in the sticking probability as well as in the rotational alignment in desorption as a function of the rotational quantum number, thus explaining recent experimental results. In addition, we have analysed the effect of the surface corrugation and the influence of the isotope on the rotational alignment in desorption.

I. Introduction

The study of gas–surface dynamics is an important field of surface science. The dynamics of the interacting particles is governed by the underlying potential energy surface (PES). However, the PES is not directly accessible by experiment. In fact, only the consequences of the PES on adsorption probabilities and desorption distributions can be measured. On the other hand, modern electronic structure methods provide a reliable tool to determine potential energy surfaces, but in order to directly compare to experiment dynamical simulations have to be performed on the theoretically determined potentials.[1]

In particular, the dynamics of the interaction of hydrogen with metal surfaces is well-studied, both experimentally[2–12] and theoretically.[1,13,14] Insight into the dynamics of the adsorption process can be obtained by using molecular beam techniques to study the dependence of the adsorption probability on kinetic energy E_i, angle of incidence Θ_i, and initial quantum conditions of the beam. For the time-reverse process, the desorption, state-specific detection of the desorbing molecules by laser techniques provides detailed information on the desorption dynamics.

While the interaction of hydrogen with copper serves as the benchmark system for activated adsorption,[4,5,12–17] the H_2/Pd system provides the standard system for the study of non-activated adsorption.[1,2,8–11,18–20] The potential energy surface of the interaction of hydrogen with Pd(100) has non-activated paths towards dissociative adsorption and no molecular adsorption well.[21] However, the majority of pathways towards dissociative adsorption have in fact energy barriers with a rather broad distribution of heights and positions, *i.e.* the PES is strongly anisotropic and corrugated.

A theoretical description of the dissociation dynamics of hydrogen on surfaces requires a quantum treatment due to the small mass of hydrogen. On the other hand, due to the large mass mismatch between hydrogen and metal substrate atoms the energy transfer from hydrogen to the substrate atoms can usually be neglected.[1,14] In the rotational excitation of H_2 scattered from Pd(111), a strong surface temperature dependence has been observed,[22] but only at incident energies that are smaller than the energy necessary for the rotational excitation, *i.e.* for a situation in which the rotational excitation would be impossible without energy transfer from the surface. These findings have been confirmed in dynamical simulations in which the moving substrate was modelled by a single surface oscillator.[23,24] In this study we are not concerned with the rotational excitation in scattering but rather with the rotational effects in the dissociation on Pd(100) which is governed by the topology of the PES. In this context the surface phonons can safely be neglected.

The role of electronic excitations for the interaction of hydrogen with metal surfaces is still rather unclear. Although the excitation of electron–hole pairs at metal surfaces upon the adsorption of hydrogen has been observed,[25] they usually correspond to a minority channel as far as inelastic effects in adsorption are concerned.[26] Hence it is also justified to neglect them for the purpose of the present study.

The dynamics of the interaction of H_2 with Pd(100) had already been the subject of theoretical studies in which all six degrees of freedom of the hydrogen molecule were treated quantum dynamically.[18,27,28] The underlying potential energy surface that was used was derived from *ab initio* total-energy calculations.[21] Experimental results for many nonactivated systems such as H_2/Pd(100) show a non-monotonic variation of the dissociative adsorption probability: with increasing energy it decreases, passes through a minimum and then increases.[2] The current understanding of this behaviour is based on the high-dimensional quantum dynamical simulations:[18,28] dynamical steering is responsible for the initial decay at low energies while static arguments invoking the barrier distribution[29] prevail at high energies. In the steering regime, the molecules do not neccessarily directly stick, but may be first dynamically trapped for a while[19,30] before they dissociate.

In addition, the stereodynamics of the associative desorption of H_2/Pd(100) have been investigated in great detail, both experimentally[8,31,32] as well as theoretically.[18,33,34] By determining the rotational alignment of desorbing hydrogen molecules, a preference for molecules rotating in the so-called helicopter mode was observed, *i.e.* for molecules with their rotational axis perpendicular to the surface which correspond to the molecular axis parallel to the surface. This could be directly related to the topology of the relevant PES since the polar anisotropy of the PES is significantly larger than the azimuthal anisotropy.

 DOI: 10.1039/b203310k

The present study was motivated by an unresolved issue that still remained in the comparison between experimental and theoretical results for the rotational aligment. The experiment showed a non-monotonic behaviour of the rotational alignment as a function of the rotational quantum number: first the rotational aligment increased, but for higher rotational quantum numbers it decreased again corresponding to an almost isotropic rotational distribution.[8,31] The high-dimensional quantum studies had been limited to rotational quantum numbers $j \leqslant 6$ because of the immense computational effort associated with larger basis sets. However, the theoretical results showed no indication of any non-monotonic behaviour as far as the dependence on the rotational state was concerned.[27,33,34]

We have therefore performed a quantum dynamical coupled-channel study[35] of the rotational effects in the system H_2/Pd(100) on a model PES that was derived from *ab initio* data. By first performing a vibrationally adiabatic fixed-site calculation we could identify the mechanism that leads to the non-monotonic dependence of the rotational alignment. Furthermore we studied isotope effects in the dissociation dynamics and checked the relevance of our results by extending the calculations to vibrationally adiabatic five-dimensional calculations in which the lateral hydrogen degrees of freedom were also considered.

In Section II we will outline the details of our computational method and motivation for the choice of the potential energy surface. In Section III we will discuss our computational results for the sticking probability as a function of the initial rotational state and derive the consequences for the rotational alignment in desorption. The paper ends with some concluding remarks.

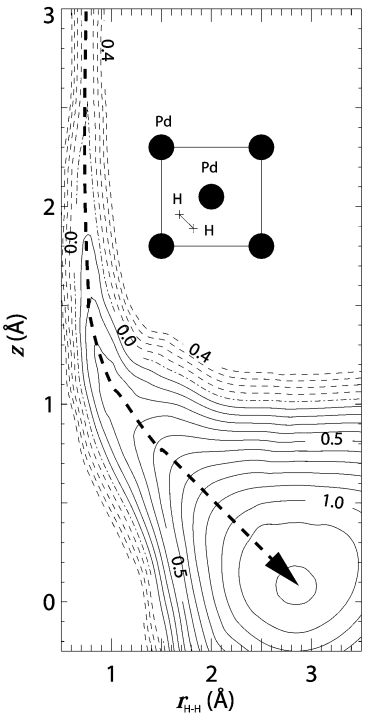

Fig. 1 Two-dimensional cut through the six-dimensional potential energy surface of H_2/Pd(100) obtained by density functional calculations.[21] The coordinates in the figure are the H_2 center-of-mass distance from the surface z and the H–H interatomic distance r. Energies are in eV per H_2 molecule. The contour spacing is 0.1 eV. The lateral coordination and the orientation of the molecule are illustrated in the inset. The dashed line corresponds to the reaction path.

II. Computational details

The potential energy surface of H_2/Pd(100) has been mapped out in great detail by density functional theory (DFT) calculations.[21] In Fig. 1 a two-dimensional cut through the six-dimensional *ab initio* PES as a function of the H_2 center-of-mass distance from the surface z and the H–H interatomic distance r is shown. The plotted cut corresponds to the most favorable reaction path. The DFT results had been used to obtain an analytical parametrization of the PES on which six-dimensional quantum dynamics calculations have been performed.[18,28]

For the present study, we have used the parametrization of the most favourable adsorption path shown in Fig. 1 from refs. 18 and 28. However, in order to investigate the influence of the other degrees of freedom on the dissociation dynamics in a more transparent way we have modified and simplified the dependence of the PES on the lateral coordinates and the orientation of the molecule.

The molecular center is referred to by (x,y,z) in a cartesian coordinate system centered on a surface atom with the z axis perpendicular to the surface. The molecular axis is defined by its length r and the polar and azimuthal angles θ and ϕ. In order to solve the time-independent Schrödinger equation for the hydrogen molecule interacting with the surface reaction path coordinates are employed. The reaction path coordinate s is defined as the coordinate along the dashed line in Fig. 1. Note that for the proper definition of the reaction path coordinate mass-scaled coordinates have to be employed, *i.e.* the interatomic distance r has been scaled by a factor of $\sqrt{\mu/M}$ where μ is the reduced mass and M the total mass of the hydrogen molecule. In fact, Fig. 1 is plotted using the corresponding scales for the z and the r axes. Throughout our study we have treated the dissociation dynamics as vibrationally adiabatic, *i.e.*, we have assumed that the vibrations perpendicular to the reaction path coordinate s in the zr-plane follow the motion adiabatically. This assumption is well-justified, as has already been demonstrated,[36] due to the fact that the vibrational coordinate corresponds to the fastest degree of freedom in the dissociation dynamics. Furthermore, the substrate atoms are assumed to be fixed since, due to the large mass mismatch between adsorbate and substrate, there is only little energy transfer.

We have first studied the rotational effects in the adsorption and desorption dynamics in fixed-site three-dimensional calculations. In this restricted geometry the PES is given in the following form:

$$V(s,\theta,\phi) = V_{\mathrm{reac}}(s) + V_{\mathrm{vib}}(s) + V_{\mathrm{rot}}(s)\cos^2\theta + \frac{1}{2}V_{\mathrm{azi}}(s)(1+\sin^2\theta\cos 2\phi). \quad (2.1)$$

Here $V_{\mathrm{reac}}(s)$ is the potential along the minimum energy path, and $V_{\mathrm{rot}}(s)$ and $V_{\mathrm{azi}}(s)$ determine the anisotropy of the PES in the polar and azimuthal orientation, respectively. Their dependence on s is parametrized as

$$V_{\mathrm{reac}}(s) = F(\tanh\lambda s - 1) \quad (2.2)$$

$$V_{\mathrm{rot}}(s) = \frac{1}{2}V_{\mathrm{pol}}(1-\tanh\lambda s) \quad (2.3)$$

$$V_{\mathrm{azi}}(s) = \frac{1}{2}V_{\mathrm{azim}}(\cosh\gamma(s-s_{\mathrm{azi}}))^{-2}. \quad (2.4)$$

The constant F is related to the adsorption energy E_{ad} by $F = \frac{1}{2}E_{\mathrm{ad}}$. The length scale of the minimum energy path is given by λ. The parameters V_{pol} and V_{azim} determine the maximum polar and azimuthal anisotropy.

Although we do not treat the molecular vibrations explicitly, we still take the change of the vibrational frequency along the reaction path into account *via* the term

$$V_{\mathrm{vib}}(s) = \hbar\omega_{\mathrm{gas}}\{1 - n(1-\tanh\gamma(s-s_{\mathrm{vib}}))\}. \quad (2.5)$$

The factor n gives the relative change of the vibrational frequency along the reaction path. This number $n = 0.38$ is actually the same as used in the six-dimensional quantum calculation,[28] *i.e.*, the vibrational frequency drops to 24% of its gas phase value along the reaction path.

These terms then enter the three-dimensional Hamiltonian

$$H_{3D} = -\frac{\hbar^2}{2M}\frac{\partial^2}{\partial s^2} + \frac{\hbar^2}{2\mu}\frac{\hat{L}^2}{r_e(s)^2} + V(s,\theta,\phi), \qquad (2.6)$$

where $\hat{L}$ is the angular momentum operator. M is the total mass of the hydrogen molecule, while μ is the reduced mass. $r_e(s)$ is the equilibrium hydrogen bond length along the reaction path. In the gas phase it is given by the hydrogen bond length 0.74 Å, but upon dissociative adsorption it increases according to Fig. 1. This means that the moment of inertia $\mu r_e(s)^2$ also increases significantly along the reaction path.

In order to have a more realistic description of the hydrogen dissociation dynamics on Pd(100) we have extended our calculations and also taken the lateral degrees of freedom of the molecule into account. The five-dimensional potential energy surface including corrugation is given by

$$\begin{aligned} V(s,\theta,\phi,x,y) = {} & V_{reac}(s) + V_{vib}(s) + V_{rot}(s)\cos^2\theta \\ & + \frac{1}{4}V_{azi}(s)(2 + \sin^2\theta\cos 2\phi \\ & \times (\cos Gx - \cos Gy)) \\ & + \frac{1}{4}V_{corr}(s)(2 + \cos Gx + \cos Gy), \end{aligned} \qquad (2.7)$$

where a is the lattice constant and $G = \frac{2\pi}{a}$ corresponds to the lattice constant of the reciprocal lattice. For V_{reac}, V_{rot} and V_{azi} we have taken exactly the same parametrization as in the three-dimensional calculations. The corrugation term V_{corr} is parametrized according to

$$V_{corr} = E_G(\cosh \gamma s)^{-2}. \qquad (2.8)$$

Here E_G is the energetic corrugation amplitude and s_{barr} the position of the barriers. This implies that we only take energetic corrugation into account and not geometrical corrugation.[13,37]

In Table 1 we have collected the most relevant parameters describing the model potential energy surface. In addition, in Fig. 2 the functions $V_{reac}(s)$, $V_{rot}(s)$, $V_{azi}(s)$ and $V_{corr}(s)$ are plotted. The five-dimensional Hamiltonian is then given by

$$\begin{aligned} H_{5D} = {} & -\frac{\hbar^2}{2M}\left(\frac{\partial^2}{\partial s^2} + \frac{\partial^2}{\partial x^2} + \frac{\partial^2}{\partial y^2}\right) \\ & + \frac{\hbar^2}{2\mu}\frac{\hat{L}^2}{r_e(s)^2} + V(s,\theta,\phi,x,y). \end{aligned} \qquad (2.9)$$

The quantum dynamics is determined in a coupled-channel scheme within the concept of the local reflection matrix [LORE].[35] Within this setup, the convergence of the results with respect to the basis set has been carefully checked. Calculations have been performed with a basis set consisting of rotational eigenfunctions with quantum numbers up to $j_{max} = 14$ and parallel momentum states with maximum parallel momentum $p_{max} = 8\hbar G$.

Table 1 Potential parameters used for the representation of the three- and five-dimensional model potential energy surface of H_2/Pd(100)

F/eV	V_{pol}/eV	V_{azim}/eV	E_G/eV
0.5	2.8	1.5	0.7

λ/Å^{-1}	γ/Å^{-1}	s_{azi}/Å	s_{vib}/Å
0.9	1.2	−1.5	1.0

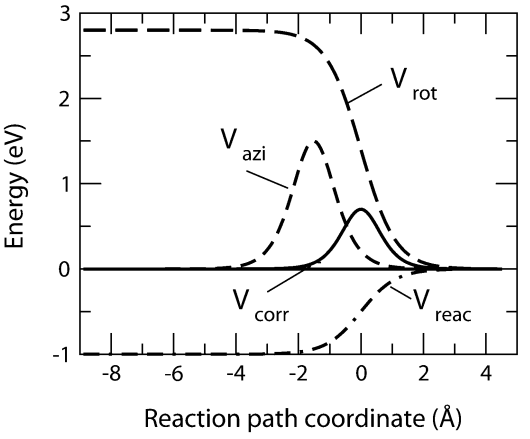

Fig. 2 The functions $V_{reac}(s)$, $V_{rot}(s)$, $V_{azi}(s)$ and $V_{corr}(s)$ describing the most favorable reaction path, the anisotropy and the corrugation of the model potential energy surface used in the calculations.

III. Results and discussions

First of all we have performed three-dimensional calculations of the sticking probability of hydrogen on Pd(100) for the center of mass of the hydrogen molecule fixed above the bridge site (see inset of Fig. 1). The D_2 results are plotted in Fig. 3 as a function of the kinetic energy for different initial rotational states. The initial states in Fig. 3(a) correspond to the so-called cartwheel rotation for which the azimuthal quantum number is $m = 0$ whereas in Fig. 3(b) results for initial helicopter rotation ($m = j$) are shown. Molecules rotating in the cartwheel fashion have their rotational axis preferentially oriented parallel to the surface so that they have a rather high probability

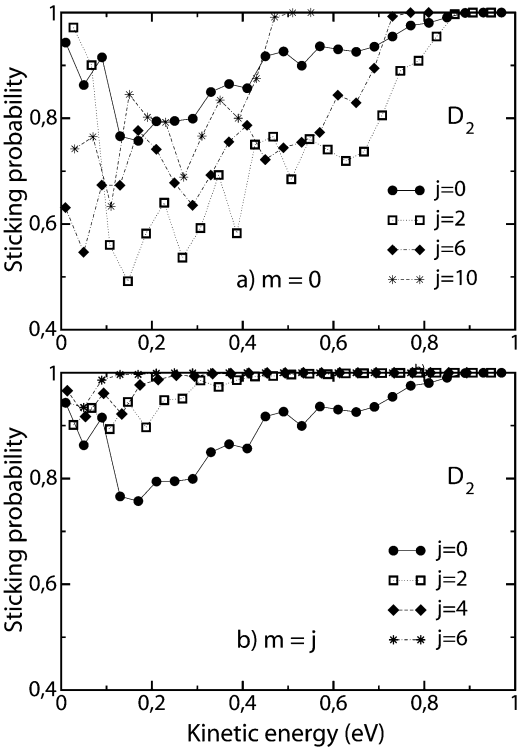

Fig. 3 Three-dimensional calculation of the sticking probability of D_2 for a range of initial rotational states j as a function of the kinetic energy. (a) Molecules initially rotating in the cartwheel fashion $m = 0$, (b) molecules initially rotating in the helicopter fashion $m = j$.

of hitting the surface in an upright fashion whereas for the helicoptering molecules the molecular axis is preferentially parallel to the surface. Note that the calculated sticking probabilities shown in Fig. 3 are larger than typical experimental values.[2,7,11] This is due to the restricted geometry of the 3D calculations in which the corrugation of the potential energy surface is not taken into account.

For the $j = 0$ states the sticking probability is governed by the steering effect:[18] At low energies, molecules impinging in an unfavourable configuration are redirected and reoriented by the anisotropy of the PES to non-activated pathways leading to the high sticking probability. This mechanism becomes less effective at higher kinetic energies where the molecules are too fast to be focused into favourable configurations towards dissociative adsorption. This causes the initial decrease in the sticking probability as a function of the kinetic energy. At even higher energies, the molecules have enough energy to directly cross the barriers, causing the sticking probability to rise again. The resonance structure in the sticking probability as a function of the kinetic energy is due to quantum mechanical threshold effects.[38–40]

Fig. 3(a) demonstrates that cartwheel rotation leads to a suppression of the sticking probability compared to the $j = 0$ non-rotating molecules. This behaviour is well known as rotational hindering:[41] rotating molecules have a smaller probability to stick since they will rotate out of a favourable orientation during the adsorption process. Furthermore, molecules rotating in the cartwheel fashion have a high probability of hitting the surface in an upright fashion for which the PES is purely repulsive.

Rotational hindering is also present for the helicopter molecules with $m = j$. However, these molecules have their axis preferentially oriented parallel to the surface which is very favourable for dissociative adsorption. This steric effect overcompensates the rotational hindering so that in fact the sticking probability increases for these molecules with increasing rotational quantum number j (see Fig. 3(b)).

A closer look at Fig. 3(a) reveals that the sticking probability is not monotonically suppressed with rising j. Actually the sticking probability first decreases from $j = 0$ to $j = 2$ and then increases again for $j = 6$ and $j = 10$. Such a non-monotonic behaviour has in fact been observed experimentally for D_2/Cu(111)[42] and H_2/Pd(111).[11] Note that the experimental results have been derived for degeneracy averaged rotational states which means that they correspond to a sum over all azimuthal quantum numbers m. For kinetic energies smaller than 0.2 eV, the calculated degeneracy averaged sticking probablities (not shown) also exhibit a non-monotonic behavior with the minimum between $j = 4$ and $j = 6$ depending on the explicit energy. Since helicopter states usually do not show a clear non-monotonic dependence on the rotational quantum number (see Fig. 3(b) or Fig. 3(a) of ref. 41 which shows the j-dependence of the reaction probability for planar rotor helicopter states for an azimuthally flat potential from analogous 3D calculations for H_2/Cu(111)), this behavior must be due to states with $m < j$. In this energy range, the degeneracy averaged sticking probablities for $j < 10$ are smaller than the $j = 0$ results, so that there is still an overall rotational hindering, which is in qualitative agreement with the experiment for the H_2/Pd(111) system[11] where, however, only sticking probabilities for j up to $j = 5$ have been determined.

This non-monotonic behavior has been explained by the competition between the rotational hindering and an opposing adiabatic effect due to the extension of the hydrogen bond length upon dissociation.[41] Along the reaction path, the bond length $r_e(s)$ and thus the moment of inertia $I = \mu r_e^2(s)$ increases. Consequently, the rotational energy

$$E_{\mathrm{rot}}(j) = \frac{\hbar^2 j(j+1)}{2I} \qquad (3.10)$$

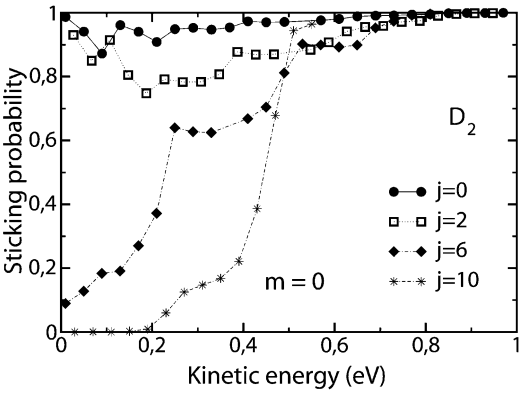

Fig. 4 Three-dimensional calculation of the sticking probability of D_2 for a range of initial rotational states j as a function of the kinetic energy for molecules initially rotating in the cartwheel fashion $m = 0$. The D–D bond length and consequently the D_2 moment of inertia are kept frozen at their gas phase values.

associated with the rotational state decreases. Assuming that the dissociation occures rotationally adiabatically, *i.e.*, without any change in the rotational quantum state, this would correspond to an effective energy transfer from the rotation to the translation which increases with the rotational quantum number. Now the dissociation is certainly not rotationally adiabatic because of the large polar and azimuthal anisotropy. In order to check whether this picture of the adiabatic energy transfer still holds approximately, we repeated the three-dimensional calculations using exactly the same potential except for the moment of inertia which we kept frozen at its gas phase value.

The results of these calculations are shown in Fig. 4 for D_2 molecules initially rotating in the cartwheel fashion. In fact, now there is a general monotonic dependence of the sticking probability on the rotational quantum number j. Enlarging the initial rotational quantum number suppresses the sticking probability so that we have the case of pure rotational hindering. This confirms that it is indeed the adiabatic rotational–translational energy transfer that is responsible for the non-monotonic behaviour of the sticking probability as a function of the rotational quantum number observed in experiment. It is the first time that this effect has been shown to be operative in a non-activated adsorption system.

Interestingly enough, while for $j = 6$ and $j = 10$ the sticking probability is strongly reduced if no change of the bond length is taken into account, for $j = 0$ and $j = 2$ the sticking probability is in fact increased. This is at first sight particularly surprising for the non-rotating $j = 0$ state where one would expect no effects due to a modification of the bond length. However, a $j = 0$ state is spherically isotropic, *i.e.*, it contains all orientations with equal weight. Since molecules with an upright orientation cannot dissociate, they have to be re-oriented before dissociation. This corresponds to the excitation of rotational motion. Quantum mechanically one would expect that for a smaller moment of inertia this excitation is suppressed since the quantum of rotational energy $E_{\mathrm{rot}}(j)$ (eqn. (3.10)) is larger. Classically, on the other hand, it is easier to re-orient an object with a smaller moment of inertia since the energy associated with a rotation with frequency ω, $E_{\mathrm{rot}}^{cl} = I\omega^2$, is proportional to the moment of inertia.

Apparently for the re-orientation of hydrogen molecules upon dissociative adsorption the classical picture is more appropriate. In order to further confirm this view we calculated the sticking probability for hydrogen molecules with a smaller constant hypothetical bond length of 0.5 Å. Indeed we found that the sticking probability for molecules in the $j = 0$ state increases even further compared to Fig. 4.

Steric effects in the rotational motion can also be observed for the time-reversed process of dissociative adsorption which is the associative desorption. Experimentally the so-called rotational alignment $A_0^{(2)}$ has been measured for hydrogen and deuterium desorbing from clean[8,12,31] and sulfur-covered surfaces.[32] The alignment parameters $A_0^{(k)}$ contain the complete dynamical information about the reaction product (or fragment). The $A_0^{(k)}$ correspond to the expectation values of the monopole, quadrupole and higher multipole moments of the angular momentum operators J:

$$A_0^0 = 1 \tag{3.11}$$

$$A_0^{(2)} = \left\langle \frac{3J_z^2 - J^2}{J^2} \right\rangle, \tag{3.12}$$

where J_z is the z-component of the angular momentum operator $\hat{J}$. The alignment parameters $A_0^{(2)}$ lie in the range

$$-1 \leqslant A_0^{(2)} \leqslant 2 \tag{3.13}$$

Molecules rotating preferentially in the cartwheel fashion have an alignment parameter $A_0^{(2)}(j) < 0$, while for molecules rotating preferentially in the helicopter fashion $A_0^{(2)}(j) > 0$.

Theoretically, the rotational alignment in desorption can directly be evaluated from the state-specific sticking probabilities $S_n(E_\perp)$ where $E_\perp$ is the normal kinetic energy and n stands for a multi-index that describes the initial vibrational, rotational and parallel momentum state of the molecule. From these sticking probabilities vibrational and rotational distributions in desorption are derived *via* the principle of detailed balance or microscopic reversibility.[36,43,44] In detail, the population D_n of the state n in desorption at a surface temperature of T_s is given by

$$D_n(E_\perp) = \frac{1}{Z} S_n(E_\perp)\, \mathrm{e}^{-\frac{E_n + E_\perp}{k_B T_s}}. \tag{3.14}$$

Here $E_\perp$ is the kinetic energy perpendicular to the surface, E_n is the energy associated with the internal state n, and Z is the partition sum that ensures the normalization of the distribution. To obtain the rotational alignment in desorption, the appropriate average over the probabilities D_n has to be performed. Since the substrate is kept fixed in the simulation, it does not participate dynamically in the adsorption/desorption process. Still it is assumed to act as a heat bath that determines the population distribution of the molecular states in desorption.

Experimentally the desorption of H_2 and D_2 from Pd(100) is characterized by positive alignment parameters showing a maximum around $j = 6$.[8,31] Six-dimensional quantum calculations of the rotational alignment so far had been limited to rotational quantum numbers $j \leqslant 6$ because of the high computational effort.[33,34] In the present work, we have therefore extended these calculations to larger rotational quantum numbers in order to qualitatively understand the measured dependence of the alignment on the rotational quantum number j. In Fig. 5, the rotational alignment derived from our three-dimensional quantum calculations is compared with the experiment for a surface temperature of $T_s = 700$ K. Our calculations show a non-monotonic behaviour of the rotational alignment as a function of the rotational quantum number; hence the qualitative trend of the experiments is reproduced. The absolute values, however, are smaller than the experimental ones. This is caused by the low dimensionality of the calculations, as will become apparent below.

As far as the isotope effect between hydrogen and deuterium is concerned, the rotational alignment for H_2 is systematically smaller than for D_2. However, it is important to note that for a given rotational quantum number j the H_2 rotational energy is twice as large as the D_2 rotational energy since the H_2 moment of inertia is only half of the D_2 value (*cf.* eqn. (3.10)). Classically, there cannot be any isotope effect as a function of the energy if all masses in a system are scaled by the same amount.[28] And in fact, the rotational alignments of H_2 and D_2 become rather similar if they are plotted as a function of the rotational energy. Hence the apparent isotope effect of the theoretical results in Fig. 5 is almost entirely due to the different rotational energies associated with the rotational quantum numbers.

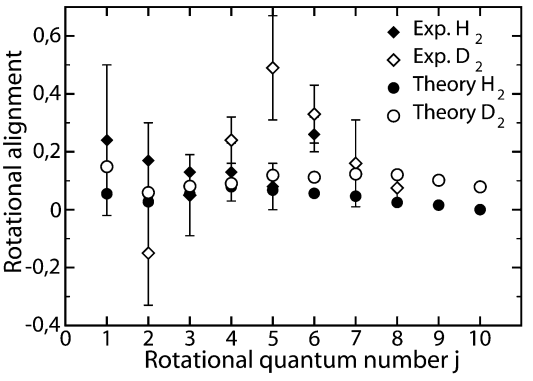

Fig. 5 Rotational alignment of H_2 and D_2 molecules desorbing from Pd(100) at a surface temperature $T_s = 700$ K. Diamonds correspond to the experimental results[8,31] while three-dimensional quantum results are plotted as circles. Filled symbols: H_2, open symbols: D_2.

The positive alignment of the desorbing hydrogen molecules is a consequence of the smaller azimuthal anisotropy of the PES compared to the polar anisotropy. For high rotational numbers, however, the difference in the sticking probabilities between cartwheel and helicopter molecules is rather small because of the adiabatic rotational–translational energy transfer. Hence it seems obvious that this adiabatic effect is also responsible for the non-monotonic behaviour of the rotational alignment. Therefore we have also determined the rotational alignment in desorption for molecules with a constant moment of inertia. And indeed, under these conditions the rotational alignment is monotonically rising, as Fig. 6 demonstrates.

In order to allow for a more realistic comparison with experiment we have additionally performed five-dimensional vibrationally adiabatic quantum calculations of the dissociation of hydrogen using the potential in eqn. (2.7). The 5D quantum results of the sticking probability for D_2 are plotted in Fig. 7. Note the different scale compared to Fig. 3. Due to the additional corrugation the sticking probability in general is suppressed compared to the three-dimensional calculations. The qualitative trends in the dependence of the sticking probability on the initial rotational state, however, are the same as in the three-dimensional calculations. For cartwheel molecules

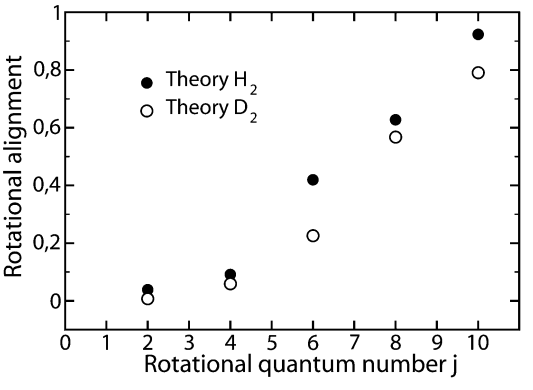

Fig. 6 Three-dimensional quantum results of the rotational alignment of hydrogen molecules desorbing from Pd(100) at a surface temperature $T_s = 700$ K with the hydrogen bond length and moment of inertia kept frozen at their gas phase values.

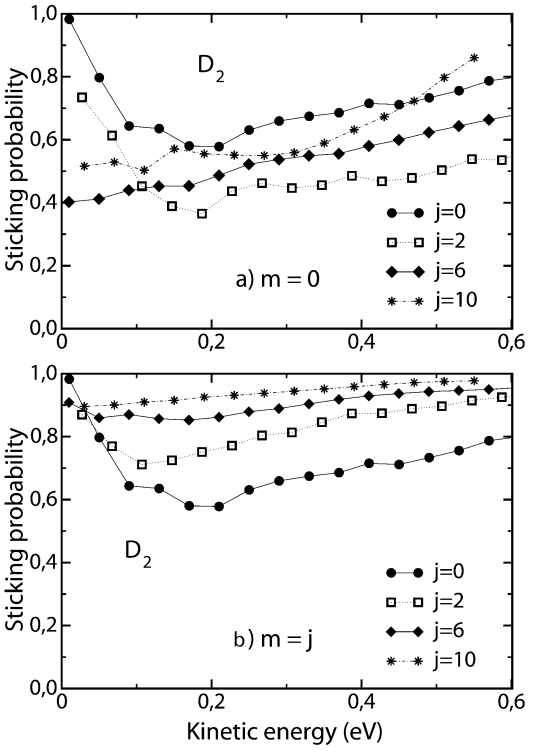

Fig. 7 Five-dimensional calculation of the sticking probability of D_2 for a range of initial rotational states j as a function of the kinetic energy under normal incidence. (a) Molecules initially rotating in the cartwheel fashion $m = 0$, (b) molecules initially rotating in the helicopter fashion $m = j$.

the sticking probability shows a non-monotonous behaviour as a function of the rotational quantum number j with the minimum for $j = 2$, while for the helicopter molecules the sticking probability rises with increasing j. Consequently, all the conclusions for the dependence of the sticking probability on the rotational state derived in the context of the three-dimensional calculations remain valid.

Furthermore, we have also determined the rotational alignment in H_2 and D_2 desorption from Pd(100) according to the five-dimensional quantum calculations. Due to the high computational effort we have only calculated microscopic transition probabilities for the manifold of even rotational and azimuthal quantum numbers.[34] Hence the rotational alignments shown in Fig. 8 correspond to an average over even m. The error associated with this approximation, however, is rather small.[34]

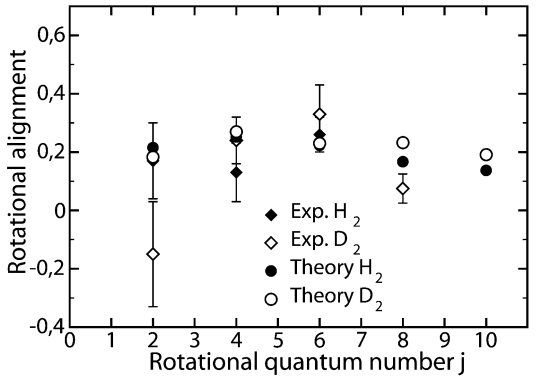

Fig. 8 Comparison of the rotational alignment of H_2 and D_2 molecules desorbing from Pd(100) at a surface temperature $T_s = 700$ K derived from five-dimensional quantum calculations (circles) with the experimental results[8,31] (diamonds). Filled symbols: H_2, open symbols: D_2.

Fig. 8 shows that the non-monotonic behaviour of the calculated rotational alignment is still reproduced, but the absolute values of the alignment are larger by a factor of about two compared to the three-dimensional calculations. The calculated values now agree satisfactorily with the experimental results. In fact, if we do not include the corrugation term in the 5D calculations, *i.e.* if we set $E_G = 0$, then the rotational alignment is very similar to the 3D case. Only when we include the rotationally isotropic corrugation V_{corr} is the rotational alignment increased by about a factor of two. This is indeed very surprising since the anisotropy of the potential energy surface is not changed by the inclusion of the term V_{corr}.

This unexpected behavior can in fact easily be understood by considering that the rotational alignment basically depends on the ratio of the desorption probabilities between helicopter and cartwheel molecules. Taking into account the corrugation term V_{corr} leads to a decrease in the adsorption and desorption probabilities that is to first order independent of the rotational state. This constant downshift, on the other hand, increases the ratio between the reaction probabilities of helicopter and cartwheel molecules, thus increasing the rotational alignment.

IV. Conclusions

We have investigated the rotational dynamics in the non-activated adsorption system H_2/Pd(100) by quantum coupled-channel calculations. The potential energy surface used is based on electronic structure calculations, but it has been simplified and adjusted in order to systematically study the influence of the topology of the potential energy surface on adsorption and desorption properties. The non-monotonic behaviour of the sticking probability and the rotational alignment in desorption observed in experiment are well-reproduced by our calculations. We have shown that this behaviour is caused by the change of the hydrogen bond length upon adsorption and desorption. For low rotational quantum numbers rotational hindering suppresses adsorption and desorption probabilities. For higher rotational quantum numbers the change in bond length along the reaction path leads to a decrease in the adiabatic rotational quantum energy which causes an effective energy transfer from rotation to translation. This effect increases the reaction probabilities and decreases the difference between the reaction probabilities of helicopter and cartwheel molecules leading to a smaller rotational alignment.

References

1 A. Groß, *Surf. Sci. Rep.*, 1998, **32**, 291.
2 K. D. Rendulic, G. Anger and A. Winkler, *Surf. Sci.*, 1989, **208**, 404.
3 H. A. Michelsen and D. J. Auerbach, *J. Chem. Phys.*, 1991, **94**, 7502.
4 C. T. Rettner, D. J. Auerbach and H. A. Michelsen, *Phys. Rev. Lett.*, 1992, **68**, 1164.
5 A. Hodgson, J. Moryl, P. Traversaro and H. Zhao, *Nature*, 1992, **356**, 501.
6 K. D. Rendulic and A. Winkler, *Surf. Sci.*, 1994, **299/300**, 261.
7 M. Beutl, M. Riedler and K. D. Rendulic, *Chem. Phys. Lett.*, 1995, **247**, 249.
8 D. Wetzig, R. Dopheide, M. Rutkowski, R. David and H. Zacharias, *Phys. Rev. Lett.*, 1996, **76**, 463.
9 D. Wetzig, M. Rutkowski, H. Zacharias and A. Groß, *Phys. Rev. B*, 2001, **63**, 205412.
10 M. Beutl, M. Riedler and K. D. Rendulic, *Chem. Phys. Lett.*, 1996, **256**, 33.
11 M. Gostein and G. O. Sitz, *J. Chem. Phys.*, 1997, **106**, 7378.
12 H. Hou, S. J. Gulding, C. T. Rettner, A. M. Wodtke and D. J. Auerbach, *Science*, 1997, **277**, 80.

13 G. R. Darling and S. Holloway, *Rep. Prog. Phys.*, 1995, **58**, 1595.
14 G.-J. Kroes, *Prog. Surf. Sci.*, 1999, **60**, 1.
15 A. Groß, B. Hammer, M. Scheffler and W. Brenig, *Phys. Rev. Lett.*, 1994, **73**, 3121.
16 G.-J. Kroes, E. J. Baerends and R. C. Mowrey, *Phys. Rev. Lett.*, 1997, **78**, 3583.
17 D. A. McCormack and G.-J. Kroes, *Phys. Chem. Chem. Phys.*, 1999, **1**, 1359.
18 A. Groß, S. Wilke and M. Seheffler, *Phys. Rev. Lett.*, 1995, **75**, 2718.
19 A. Groß and M. Scheffler, *J. Vac. Sci. Technol. A*, 1997, **15**, 1624.
20 H. F. Busnengo, W. Dong and A. Salin, *Chem. Phys. Lett.*, 2000, **320**, 328.
21 S. Wilke and M. Scheffler, *Phys. Rev. B*, 1996, **53**, 4926.
22 E. Watts and G. O. Sitz, *J. Chem. Phys.*, 1999, **111**, 9791.
23 H. F. Busnengo, W. Dong, P. Sautet and A. Salin, *Phys. Rev. Lett.*, 2001, **87**, 127601.
24 Z. S. Wang, G. R. Darling and S. Holloway, *Phys. Rev. Lett.*, 2001, **87**, 226102.
25 B. Gergen, H. Nienhaus, W. H. Weinberg and E. W. McFarland, *Science*, 2001, **294**, 2521.
26 J. T. Kindt, J. C. Tully, M. Head-Gordon and M. A. Gomez, *J. Chem. Phys.*, 1998, **109**, 3629.
27 A. Groß, S. Wilke and M. Scheffler, *Surf. Sci.*, 1996, **357/358**, 614.
28 A. Groß and M. Scheffler, *Phys. Rev. B*, 1998, **57**, 2493.
29 M. Karikorpi, S. Holloway, N. Henriksen and J. K. Nørskov, *Surf. Sci.*, 1987, **179**, L41.
30 C. Crespos, H. F. Busnengo, W. Dong and A. Salin, *J. Chem. Phys.*, 2001, **114**, 10 954.
31 D. Wetzig, M. Rutkowski, R. Etterich, W. David and H. Zacharias, *Surf. Sci.*, 1998, **402**, 232.
32 M. Rutkowski and H. Zacharias, *Phys. Chem. Chem. Phys.*, 2001, **3**, 3645.
33 A. Groß and M. Scheffler, *Prog. Surf. Sci.*, 1996, **53**, 187.
34 A. Eichler, J. Hafner, A. Groß, and M. Scheffler, *Chem. Phys. Lett.*, 1999, **311**, 1.
35 W. Brenig, T. Brunner, A. Groß and R. Russ, *Z. Phys. B*, 1993, **93**, 91.
36 A. Groß and M. Scheffler, *Chem. Phys. Lett.*, 1996, **256**, 417.
37 A. Groß, *J. Chem. Phys.*, 1995, **102**, 5045.
38 A. Groß and M. Scheffler, *Chem. Phys. Lett.*, 1996, **263**, 567.
39 A. D. Kinnersley, G. R. Darling, S. Holloway and B. Hammer, *Surf. Sci.*, 1996, **364**, 219.
40 A. Groß, *J. Chem. Phys.*, 1999, **110**, 8696.
41 G. R. Darling and S. Holloway, *J. Chem. Phys.*, 1994, **101**, 3268.
42 H. A. Michelsen, C. T. Rettner, D. J. Auerbach and R. N. Zare, *J. Chem. Phys.*, 1993, **98**, 8294.
43 H. J. Kreuzer and Z. W. Gortel, *Physisorption Kinetics*, Springer Series in Surface Sciences, vol. 1, Springer, Berlin, 1986.
44 W. Brenig, *Nonequilibrium therrmodynamics*, Springer, Berlin, 1990.